Formation and Disruption of Viscoelastic Wormlike Micellar Networks in the Mixed Surfactant Systems of Sucrose Alkanoate and Polyoxyethylene Alkyl Ether

Alicia Maestro,[†] Durga P. Acharya,[‡] Hidemitsu Furukawa,[§] José M. Gutiérrez,[†] M. Arturo López-Quintela,[⊥] Masahiko Ishitobi,[||] and Hironobu Kunieda*[,‡]

Department of Chemical Engineering, Barcelona University, Martí i Franquès 1, 08028 Barcelona, Spain, Graduate School of Environment and Information Sciences, Yokohama National University, Tokiwadai 79-7, Hodogaya-ku, Yokohama 240-8501, Japan, Department of Organic and Polymer Materials Chemistry, Tokyo University of Agriculture and Technology, 2-24-16 Naka-cho, Kogane-shi, Tokyo 184-8588, Japan, Department of Physical Chemistry, University of Santiago de Compostela, E-15782 Santiago de Compostela, Spain, and Specialty Chemical Laboratory, Yokohama Research Center, Mitsubishi Chemical Co., Kamoshida-cho, Aoba-ku, Yokohama 227-8502, Japan

Received: March 23, 2004; In Final Form: July 9, 2004

Addition of lipophilic nonionic amphiphiles, such as short EO-chain polyoxyethylene dodecyl ether ($C_{12}EO_n$, $n = 1-4$) and monolaurin (ML), to the dilute micellar solution of sucrose hexadecanoate (P1695) induces a sharp increase in viscosity that is attributed to the one-dimensional micellar growth. With successive addition of the nonionics, the viscosity gradually decreases and, eventually, a phase separation occurs. In the maximum-viscosity region of the mixed systems, a viscoelastic solution with a rheological behavior typical of the interwoven network of wormlike micelles is obtained. The oscillatory shear behavior of the systems can be described by the Maxwellian model in the region of low shear frequency. The ability of the lipophilic nonionics to induce micellar growth in the mixed system decreases in the following order: ML $\approx C_{12}EO_1 \approx C_{12}EO_2 < C_{12}EO_3 < C_{12}EO_4$. A similar effect of the hydropilic group is observed in the sucrose dodecanoate (SM1200)/$C_{16}EO_n$ aqueous system, although the micellar growth is comparatively less favorable, and a sharp increase in viscosity occurs near the boundary of the micellar phase. The microstructural change with surfactant mixing ratio in the representative P1695/$C_{12}EO_4$ system, based on the results of dynamic light scattering and rheological measurements, is discussed. A change from spherical to wormlike micelles, followed by branching and further separation of branching points as disklike micelles, precursors of the lamellar liquid crystal phase, is proposed.

1. Introduction

Wormlike or threadlike micellar systems,[1−5] also named living polymers,[4,6−9] have attracted attention for both basic and practical research since they show highly viscoelastic behavior at relatively low surfactant concentration. Although the formation of wormlike structures and micellar entanglements between them, and the large increase in viscoelasticity that this phenomena produces have been extensively investigated, most of studies are related to cationic surfactant systems such as CTAB or CTAT or others with or without salts[10−19] or cationic−anionic mixtures.[20−25] Hence, the real mechanism of the wormlike formation and the enormous increase in viscosity have not been completely clarified yet. Especially, although wormlike formation has been reported in nonionic surfactant systems[26−28] there are only a few reports of highly viscoelastic systems in a dilute concentration range for nonionic surfactant systems.[29,30] Nonionic surfactant systems are expected to be highly insensitive to salt due to the absence of electrostatic interactions. They would be very good candidates for basic studies as well as practical applications, because the complicated ionic interaction does not have to be taken into account.

Recently, we found that polyoxyethylene cholesteryl ether−$C_{12}EO_n$ aqueous mixtures show an enormous increase in viscosity in a rather dilute region.[29] The packing of rigid cholesteryl rings and C_{12} chains causes the formation of wormlike micelles due to the optimum effective sectional area by mixing. Namely, the average effective cross-sectional area decreases by replacing the large area of hydrophilic cholesteryl surfactant with a small lipophilic conventional nonionic surfactant. Until certain mixing fractions of $C_{12}EO_n$, the viscosity does not greatly increase, but when the effective cross-sectional area reaches the optimum, a dramatic increase in viscosity is observed.

Sucrose alkanoates, derived from sugar and vegetable oils, are nontoxic, biodegradable, and biocompatible properties that make them suitable for use as emulsifiers in the food industry, cosmetics, and pharmaceutical formulations.[31] They have unique features such as formation of temperature-insensitive microemulsions, and highly concentrated emulsions.[32−35] They form spherical micelles in the dilute region. Hence, a sphere−rod transition of micelles is expected by mixing them with a lipophilic nonionic surfactant with a small head. As a result, these kinds of surfactants would form a highly viscoelastic system in the dilute region.

In this article we report the formation of the viscoelastic micellar phase due to the presence of wormlike micelles in mixed systems of sucrose alkanoates and short-chain polyoxyethylene alkyl ether type nonionic surfactants. Rheological

* Corresponding author. Fax: +81-45-339-4190. E-mail: kunieda@ynu.ac.jp.
[†] Barcelona University.
[‡] Yokohama National University.
[§] Tokyo University of Agriculture and Technology.
[⊥] University of Santiago de Compostela.
[||] Mitsubishi Chemical Co.

10.1021/jp048716u CCC: $27.50
Published on Web 08/24/2004

results are compared with dynamic light scattering (DLS) experiments. We also study the influence of the headgroup and the amphiphile/sucrose ratio, maintaining constant the total concentration of surfactant, which ensures that the change in behavior is related to changes in the shape of micelles and not due to an increase in concentration.

2. Experimental Section

2.1. Materials. Reagent grade sucrose dodecanoate (monoester content >95%), abbreviated as SM1200, and sucrose hexadecanoate (monoester content >93.6%), named here P1695, were supplied by Mitsubishi Chemical Co. (Japan). Monolaurin (ML) (98%) was supplied by Tokio Kasei Kogyo Co. Ltd. (Japan). Polyoxyethylene dodecyl and hexadecyl ethers (abbreviated as C_mEO_n, $m = 12$ or 16 and $n = 1$, 2, 3 and 4) were purchased from Nikko Chemicals Co. (Japan). All chemicals were used without further purification. Millipore-MilliQ water was used in the preparation of the samples.

2.2. Phase Diagrams. All chemicals were weighed and sealed in ampules. After being properly mixed at relatively high temperature, samples were kept at 30 °C during the time required for equilibration. The phase change was identified by direct visual inspection and with crossed polarizers for birefringence.

2.3. Rheological Measurements. Samples for rheological measurements were prepared by addition of the desired amount of water and each amphiphile to a weighted amount of sucrose surfactant mother solution of the proper concentration. The samples were stirred and slightly heated to homogenize them. After that solutions were stored at 30 °C for at least 48 h before use to ensure equilibration. Rheological measurements were performed with an ARES rheometer (Rheometrics Scientific) at 30 °C to avoid precipitation of P1695, since the Kraft temperature of this surfactant is around room temperature. Three different sensors were used, depending on the viscoelasticity range of the solutions. A Couette geometry with cup diameter 34 mm, bob diameter 32 mm, and bob length 33.3 mm was used for the less viscoelastic samples, and cone-and-plate sensors of 50 and 25 mm in diameter, both with a cone angle of 0.04 rad, were used for middle and high viscoelastic samples, respectively. A device to avoid evaporation was installed. Some measurements were carried out with two sensors and results were compared to ensure that experimental data were not influenced by them. Oscillatory frequency sweep measurements were carried out at a strain of 10% for working in the linear viscoelastic region. This strain was selected through preliminary dynamic strain sweep measurements. Steady-state curves were obtained by using the control shear rate mode. Shear rate sweeps were used, the time for each shear rate being long enough to ensure the achievement of steady state.

2.4. DLS Measurements. Solutions used to prepare the samples for DLS measurements were filtered through a Minisart syringe filter with a mesh size of 0.2 μm (Sartorius, Germany) to obtain dust-free samples. DLS measurements were performed with a scanning microscopic light scattering apparatus.[36,37] By using this apparatus, it is possible to overcome the problem concerning the anomalous scattering from static and dynamic inhomogeneities in samples and rigorously determine the ensemble-averaged correlation function. In this study, a light-scattering cell (glass tube) of 5 mm outer diameter was used. The temperature was controlled at 30.0 °C. The sample tube was moved by stepping motor with a 1-μm step. For each sample, the time-averaging measurements were first held at 20 different positions. By averaging them, we finally determined the ensemble-averaged correlation function. Then, the distribution function of the relaxation time of the dynamic fluctuation $P(\tau_R)$ was calculated from the ensemble-averaged correlation function, $\Delta g_{en}^{(1)}(\mathbf{q},\tau)$, by inverse Laplace transformation. The details on the DLS measurement were reported in a previous study.[36]

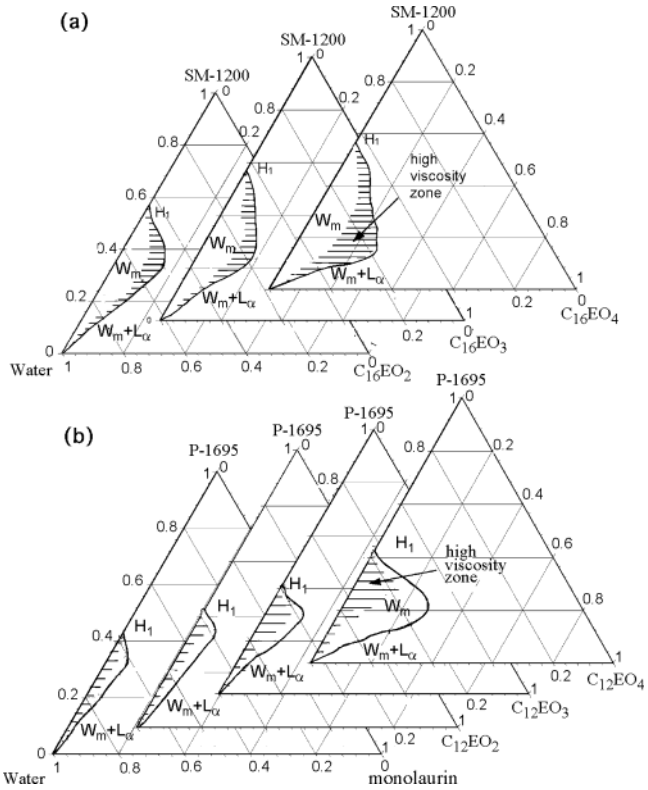

Figure 1. Phase diagram of (a) SM1200−water−$C_{16}EO_n$ and (b) P1695−water−$C_{12}EO_n$ systems at 30 °C. W_m is the micellar phase, and H_1 and L_α are the hexagonal and lamellar liquid crystalline phases, respectively.

3. Results

3.1. Phase Behavior. A partial phase diagram of P1695−$C_{12}EO_n$−water, P1695−ML−water, and SM1200−$C_{16}EO_n$−water systems in the dilute region is shown in Figure 1a,b. Although only the micellar region (W_m) boundary was determined with accuracy, we roughly observed that successive addition of C_mEO_n or ML to the micellar phase of sucrose alkanoate−water binary systems produces a phase transition from W_m to hexagonal liquid crystal (H_1) at high sucrose alkanoate concentrations whereas a W_m−lamellar liquid crystal (L_α) phase transition takes place at low concentration, due to the decrease in surfactant layer curvature produced by the incorporation of the amphiphile.[32] A region of high viscosity, roughly drawn by the shaded area, is visually observed inside the W_m phase for all the cases. This region is reached with the first drop of $C_{12}EO_n$ or ML in the P1695 solutions (Figure 1b), and a highly viscoelastic or gellike behavior is observed that is maintained in an interval of concentrations and progressively disappears with further addition of $C_{12}EO_n$, before the phase separation. These highly viscous samples show shear birefringence. For the SM1200 solutions, a higher amount of $C_{16}EO_n$ is required for a significant increase of viscosity that is maintained up to phase separation. However, the solutions obtained are much less viscoelastic than that obtained with P1695. An increase of n in C_mEO_n shifts the mentioned W_m

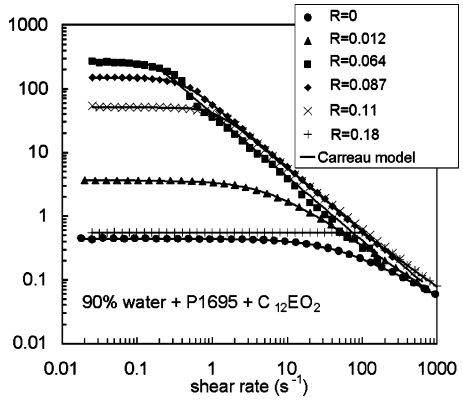

Figure 2. Viscosity vs shear rate for the system water−P1695−$C_{12}EO_2$ at 90% water and various ratios of $C_{12}EO_2$/P1695.

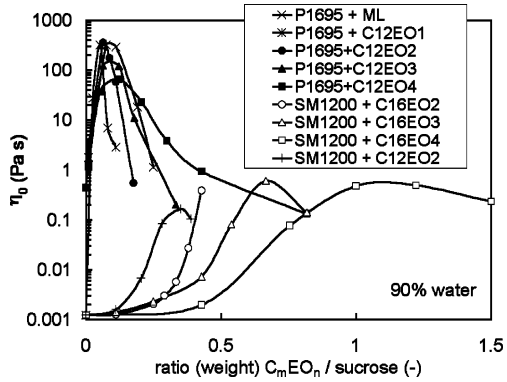

Figure 3. Zero shear viscosity for several mixed systems (water content 90%).

and viscous areas to higher concentrations of the ethoxylated amphiphile for both sucrose esters, as can be seen in Figure 1.

3.2. Rheology. *Steady-State Viscosity.* Shear rate sweep tests were made to obtain the steady-state viscosity for all the systems shown in the phase diagrams, and also with P1695+$C_{12}EO_1$, all in the W_m zone, at 95% and 90% water. An example can be seen in Figure 2 for 90% water and several ratios (R) of $C_{12}EO_2$/P1695. Shear thinning behavior is observed for all the samples. All results obtained with P1695 can be fitted to the Carreau model, in such a way that zero shear viscosity (η_0) can be estimated. Behavior is Newtonian at small shear rates, and it starts to be shear thinning at intermediate shear rates, with a slope of −1. Samples with a higher η_0 behave as shear thinning at a smaller shear rate, because when the system is more structured or more entangled, it is also more "rigid" and as a consequence more sensitive to the shear. Experiments made with SM1200 show a nearly Newtonian behavior in the range of shear rates studied (data not shown).

Figure 3 shows the η_0 obtained through the fitting of the steady state curves to the Carreau model. It can be observed that viscosity quickly increases in several orders of magnitude if a small amount of the amphiphile is added to P1695 and then progressively decreases at higher ratios R up to phase separation. The maximum is reached at a lower R when the end cap of the amphiphile is smaller, and the value of this maximum is also higher, that is ML $\approx$ $C_{12}EO_1$ $\approx$ $C_{12}EO_2$ > $C_{12}EO_3$ > $C_{12}EO_4$. The same behavior is observed when working with SM1200, although the increase in η_0 takes place at higher R and, moreover, the maximum value is much smaller in these cases. The same results can be qualitatively observed when working at 95% water, the maximum on viscosity being obtained around the same R as at 90% water, but the values are lower (data not shown).

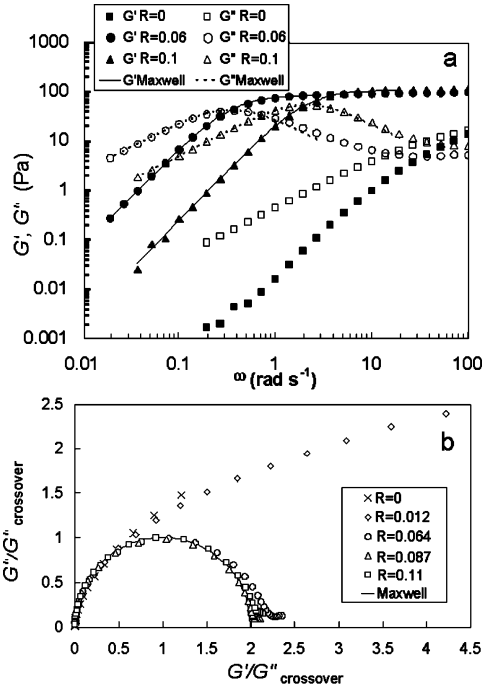

Figure 4. Frequency sweep measurements at several ratios of $C_{12}EO_2$/P1695, R (water 90%): (a) G' and G'' vs frequency; (b) Cole−Cole plots.

Oscillatory Measurements. Frequency sweep tests were carried out with all the samples prepared at 95% and 90% water and several ratios of amphiphile/sucrose (R). An example is shown in Figure 4 for 90% water−$C_{12}EO_2$−P1695 systems. A non-Maxwellian behavior with poor viscoelasticity is observed in solutions of pure P1695 (Figure 4a). Around a certain R the sample is highly viscoelastic and storage and loss moduli, G' and G'', can be fitted to a single Maxwell model in the range of small and intermediate frequencies. This pattern is characteristic of wormlike micelles. The viscoelasticity response increases up to an optimum ratio that corresponds to the maximum in η_0 shown in Figure 3. At higher R the crossing point moves to higher frequencies, indicating a smaller relaxation time and, as a result, a poorer viscoelasticity. At very high R the Maxwellian behavior is completely lost, indicating that the relaxation process is now due to a different mechanism, and the relaxation time is so short that it cannot be observed through rheological measurements. Data are shown in a normalized Cole−Cole plot[17] in Figure 4b, where it can be seen that at $R = 0$ and high R the shape of the curves is very far from a semicircle, as it should to be if it followed the Maxwell model.

3.3. DLS Measurements. DLS measurements were performed for water−P1695−$C_{12}EO_4$ systems at 90% water and several ratios of $C_{12}EO_4$/P1695. Some results are shown in Figure 5.

Two or three relaxation modes are found depending on the composition. In Figure 5a the relaxation spectra of a sample with $R = 0.1$ is shown. The fast mode (fm) is the most important one and dominates over the medium (mm) and slow (sm) modes. This is typical for systems with $R \leq 0.5$. At higher R values the relaxation spectra change and the medium mode becomes more important, as can be seen in Figure 5b, corresponding to a sample with $R = 0.3$. Above $R = 0.7$, the medium mode becomes the most important one. This change in behavior can be more clearly seen in Figure 6, which shows the intensity amplitude ratio for the fast and medium modes. The intensity of the two modes becomes identical for a ratio $R \approx 0.65$. At this point both the static and the dynamic components of the

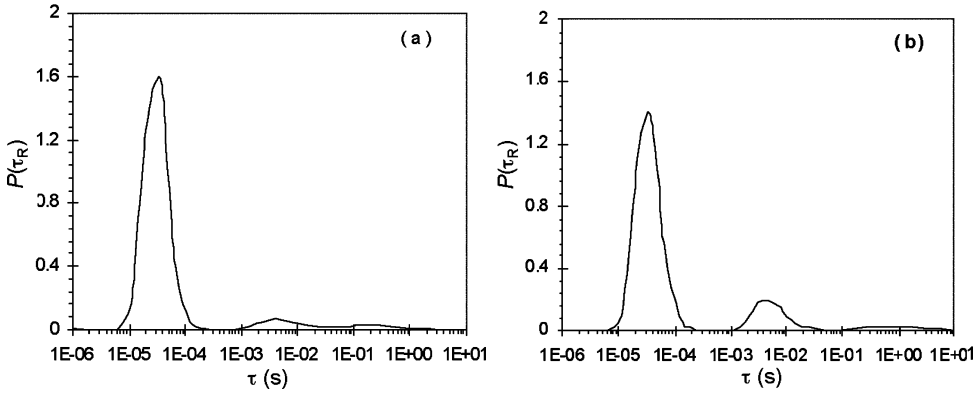

Figure 5. Relaxation spectra for water−P1695−$C_{12}EO_4$ systems at 90% water at $C_{12}EO_4$/P1695 ratio: $R = 0.1$ (a) and 0.3 (b).

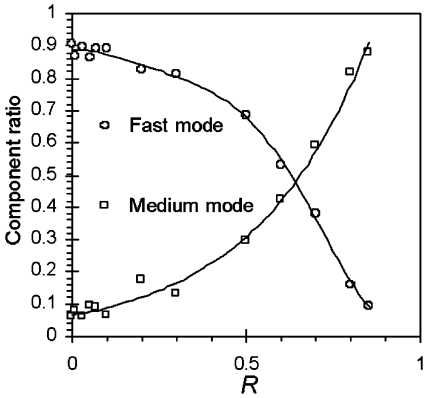

Figure 6. Intensity−amplitude ratio for fast and slow modes at various $C_{12}EO_4$/P1695 ratios (R) in water−P1695−$C_{12}EO_4$ systems at 90% water.

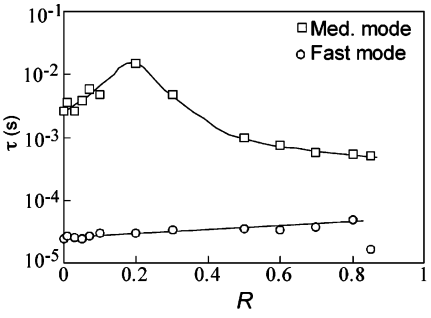

Figure 7. Variation of relaxation time (τ) for the slow and fast modes for water−P1695−$C_{12}EO_4$ systems at 90% water as a function of $C_{12}EO_4$/P1695 ratio (R).

scattering intensity (results not shown) begin to increase, mainly due to the increase of the medium mode. In Figure 7 it is shown how the average relaxation times of the fm and mm modes change with R. It can be observed that the fast mode remains nearly constant, in the range of R values, whereas on the contrary, the medium mode first increases until $R \approx 0.2$ and then decreases. It can be seen that the medium mode follows the same tendency of the viscosity and viscoelasticity shown in Figures 3 and 4, whereas the fast mode does not "feel" the change in the viscoelastic properties of the system. This result is in agreement with previous DLS results in gels[38] showing that the fm mode does not appreciably change upon gelation, whereas the mm mode, which can be associated with the formation of clusters, can be considered as a good sensor of the macroscopic viscosity.[38] The third, nondiffusive slow mode can be related to the formation of a transient network,[38] and appears only in a determinate region of R values: $R \approx 0.05-0.4$.

4. Discussion

4.1. Influence of Amphiphile Headgroup and Sucrose Alkanoate Lipophilic Tail Size. Figure 3 shows that, when working with the same sucrose alkanoate, if n of C_mEO_n is decreased (i.e. the size of the headgroup is smaller), a lower R is required to reach the maximum viscosity. Moreover, the value of the maximum is higher when n is smaller. This implies that C_mEO_n induce micellar growth more easily when the headgroup is small. According to this micellar growth, the Maxwellian behavior observed in the P1695−$C_{12}EO_2$ systems (Figure 4) is typical of that of entangled wormlike micelles.[29] It can also be seen in Figure 1 that the micellar phase zone W_m is narrower at lower values of n, indicating that transition to the flat surface or curvature zero occurs earlier. On the other hand, if the lipophilic tail of the sucrose is changed from C_{12} to C_{16}, the increase in viscosity occurs at much smaller ratios. Then, a much lower proportion of C_mEO_n is required to produce cylindrical micelles long enough to overlap and entangle and, as a result, increase the viscoelasticity of the system. The values of η_0 are also much higher when P1695 is used (Figure 3). These results can be explained through the packing parameter, $p = v/a_s l$, with l and v being the length and the volume of the lipophilic tail and a_s the cross-sectional area of the headgroup at hydrophobic interface. This parameter determines the interfacial curvature of the aggregate.

If a_s is big compared to v, as occurs with sucrose alkanoate surfactants, micelles tend to be spherical or very slightly elongated, because the tails are packed in the core of the aggregate but the headgroups need a big surface to be accommodated and, as a result, a high curvature is required at the interface. When C_mEO_n, which contains a much smaller headgroup, is added, it forms mixed micelles with the sucrose surfactant, in such a way that, as its a_s is smaller, the mean a_s of the mixed micelle is reduced and the curvature decreases, inducing transition from spherical to rodlike micelles and, after that, growth of rodlike micelles into giant wormlike micelles, to reduce the proportion of endcaps, with higher curvature.[29] Of course, by reducing n, i.e., the size of the headgroup, the effect of C_mEO_n on curvature is more important and can be observed at smaller ratios. On the other hand, as SM1200 has a smaller tail than P1695, its v is also smaller and the tails need less space to be accommodated, increasing curvature. So, a higher ratio R is required to produce an effect in curvature strong enough to induce one-dimensional growth of micelles.

A Newtonian behavior is observed for all samples with SM1200 at the concentrations of 90% and 95% water used, and only at higher concentrations of total surfactant does a slight shear thinning behavior start to appear. It corroborates the idea that elongation of micelles is less favored with SM1200 than

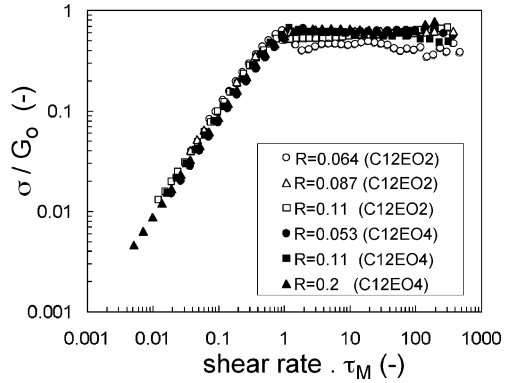

Figure 8. Reduced shear stress vs reduced shear rate for water−P1695−$C_{12}EO_2$ or $C_{12}EO_4$ at several ratios.

with P1695. Figure 2 shows that the steady-state behavior of water−P1695−$C_{12}EO_2$ systems is extremely shear thinning, especially at ratios around the maximum of η_0. In fact, the slope −1 indicates a limit in the shear thinning behavior, as can be seen in Figure 8, where data are presented as reduced shear stress (σ/G_0) vs reduced shear rate ($\dot{\gamma}\tau_M$), the plateau modulus G_0 and the relaxation time τ_M being calculated independently from oscillatory measurements. It can be observed that a plateau is reached in shear stress, named *saturating stress*, around a critical shear rate $\approx 1/\tau_M$, which leads to shear-banded flow, typical of wormlike micelles.[39,40] Higher shear rates do not increase the shear stress applied to the sample. A stronger shear thinning would imply a decrease in shear stress with an increase in shear rate, indicating that the shear flow in this region is unstable. Moreover, if different water−P1695−$C_{12}EO_n$ systems are represented together (Figure 8), all of them collapse at a saturating stress $\approx 0.6G_0$, slightly smaller than the $0.67G_0$ predicted by the model proposed by Cates.[1] This extreme shear thinning may play an important role in several applications (shampoos, cosmetics, food, etc.). The change from Newtonian to shear thinning behavior with shear rate is very abrupt around the ratio R where η_0 is maximum. The shear birefringence observed in these samples, as the shear thinning behavior, can be related to the orientation of wormlike micelles in the direction of the flow.

4.2. Influence of *R*: Comparison with the Cates Model. Figures 2 and 3 show an increase in viscosity followed by a decrease with successive addition of amphiphile to the sucrose alkanoate watery system. These results are consistent with oscillatory results that can be seen in Figure 4, where Maxwellian behavior, related to the presence of highly entangled wormlike micelles, can be observed at ratios around the maximum in viscosity. This Maxwellian pattern is described by the Cates model,[4,41] which considers the reptation-reaction process of the so-called *living polymers*. The Cates model couples the diffusive disentanglement of micelles due to their reptation along a tube to the kinetic equations describing their reversible breakdown. It implies that two relaxation processes at two different time scales take place, with two characteristic relaxation times, reptation time τ_{rep} and breaking time τ_b. When $\tau_b \ll \tau_{rep}$ the viscoelastic response at low and intermediate frequencies can be fitted to a single Maxwell model with a relaxation time given by $\tau_M = (\tau_b\tau_{rep})^{0.5}$. Then, the plateau modulus follows the equation $G_0 = \eta_0/\tau_M$.

To deepen the study of the R effect on the formation of wormlike micelles, DLS experiments were carried out in water−P1695−$C_{12}EO_4$ systems at several ratios R. Some oscillatory results are shown in Figure 9 to be correlated with DLS data.

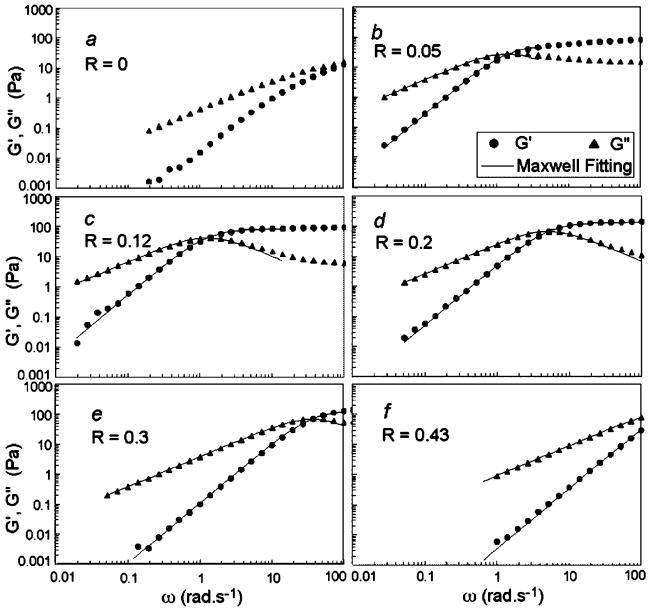

Figure 9. Frequency sweep of water−P1695−$C_{12}EO_4$ systems at several $C_{12}EO_4$/P1695 ratios, R.

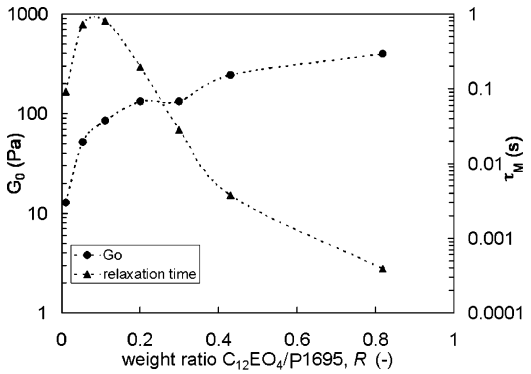

Figure 10. G_0 and τ_M vs R for the water−P1695−$C_{12}EO_4$ system.

When possible, curves at low and intermediate frequency range have been fitted to a single Maxwell model.

Values of the Maxwellian parameters G_0 and τ_M are presented in Figure 10 vs ratio R. It can be seen that G_0 increases and τ_M quickly increases and then decreases with R. The plateau modulus G_0 can be related to the mean length between entanglements, l_e, by the expression[42] $G_0 \approx kT / l_e^{9/5}$. It implies that the length between entanglements in the micellar network decreases with R or, what is the same, the number density of junctions increases. On the other hand, the maximum in relaxation time τ_M would be related to a maximum in the average micellar length $\bar{L}$. According to the Doi and Edwards theory for pure reptation[43] the reptation time τ_{rep} is proportional to $\bar{L}^3$ when total concentration is not changed. So, an increase of $\bar{L}$ would imply an increase in τ_{rep} and, as a result, in τ_M. This pattern is related to the change in the shape of micelles and the interaction between them as a consequence of the change in curvature. At very low R micelles are not elongated enough to entangle. Then, the number of entanglements can be neglected and micelles move easily, so relaxation is fast and G_0 and τ_M are small. When $C_{12}EO_4$ is added, micelles quickly grow due to the decreasing curvature, and entanglements appear, so G_0 and τ_M increase, indicating an increase in $\bar{L}$, up to a $\bar{L}$ maximum corresponding to the maximum in τ_M. Then, relaxation time decreases and the reason could be the formation of branched micelles. The existence of branched micelles, which has been demonstrated in other systems by Cryo-TEM,[7,44] is in fact the

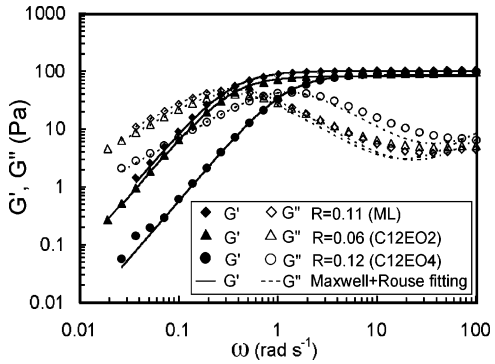

Figure 11. Fitting of several systems (90% water) to Maxwell + Rouse models.

consequence of the decreasing curvature. It would seem that the cylindrical micellar geometry provides the optimal packing conditions, and micelles should grow indefinitely, because there is no energetic incentive for branching. However, a "fusion reaction"[6] is possible, where a branch is formed by the fusion of an endcap of a micelle with the cylindrical body of another, and it can be energetically favorable because an endcap disappears. Actually, branched micelles may constitute the intermediate structures between linear micelles and bilayers, which are the precursors of the L_α liquid crystal.[17,18] Then, the effective length of micelles $\bar{L}$ decreases and τ_M is smaller, but G_0 increases since the number of junctions continues to increase, although now there are not only entanglements but also "crosslinks". In fact, in this situation the relaxation process may be faster because it can involve the fast sliding of connections along the micelles, since the surfactant monomers are not chemically connected.[19,45,46]

The single Maxwell model can fit oscillatory functions at low and intermediate frequencies, but results deviate from Maxwellian behavior at higher ones. An upturn is observed in G'', which has been attributed in other systems to a transition of the relaxation mode from reptation−scission to breathing or Rouse modes.[41,43] However, G'' does not show a clear minimum, but a very wide one followed by an upturn with increasing ω, suggesting a wide spectrum of the stress relaxation at high frequency or several relaxation processes superimposed. If the relaxation mechanism was, as in other systems, living reptation at long times + Rouse rapid relaxation, results should be fitted by eqs 1 and 2, where a Rouse relaxation mode[47] has been added to the Maxwell model, subscripts M and R referring to Maxwell and Rouse relaxations, respectively:

$$G' = G_{0,M}\frac{(\omega\tau_M)^2}{1+(\omega\tau_M)^2} + G_{0,R}\sum_{p=1}^{N}\frac{(\omega\tau_R/p^2)^2}{1+(\omega\tau_R/p^2)^2} \quad (1)$$

$$G = G_{0,M}\frac{\omega\tau_M}{1+(\omega\tau_M)^2} + G_{0,R}\sum_{p=1}^{N}\frac{\omega\tau_R/p^2}{1+(\omega\tau_R/p^2)^2} \quad (2)$$

We tried to use this model to fit results of several samples at ratios R around the maximum in viscosity or in τ_M, where maximum elongation of micelles occurs. However, it can be seen that the model predicts a more defined minimum followed by a stronger upturn of G'' (Figure 11). The same result is found if the Hess model is used, which includes the addend $\omega\eta_\infty$ in the Maxwell model for G'', with η_∞ being the viscosity at very high shear. These results support the idea that in this system other relaxation processes exist, besides the reptation−scission and the Rouse mode. This idea can be corroborated through the DLS results. The existence of an intermediate relaxation mode (mm) associated with the formation of clusters and the presence of a fast relaxation mode (fm) related to movements of monomers and spherical micelles could produce a deviation of the model proposed in eqs 1 and 2, due to the overlap of different relaxation modes at intermediate and high frequencies.

With respect to DLS results and their relation to rheological behavior, in Figure 7 we observe that the fast mode slightly increases, almost linearly, with the ratio R. The average hydrodynamic size that can be obtained from this mode changes from ≈2.4 nm for $R = 0$ to ≈7 nm at $R \approx 0.8$, but in all cases there is a broad distribution of relaxation times which clearly overlaps the range of values. Therefore we can say that this mode could correspond to the average value of monomers (and/or oligomers) and spherical micelles which seem to be present in the range of R values explored. The increase in size by increasing R then can be related to the inclusion of some $C_{12}EO_4$ molecules in these spherical micelles giving rise to slightly bigger (but yet spherical or just a little elongated!) micelles because of the reduction in curvature. In any case, the presence of this fast mode would affect rheological measurements at the highest frequencies tested.

The presence of a medium mode at $R = 0$, corresponding to sizes of ≈240 nm, could indicate the formation of micellar clusters in the pure sucrose system due, for example, to attractive forces among the terminal OH groups.

When only a small amount of $C_{12}EO_4$ is added to the system, the component ratio of the medium to fast mode increases (Figure 6), as the value of its relaxation time does (Figure 7). This fact could be explained by the growth of a portion of the spherical and slightly elongated micelles into more elongated, wormlike ones. The presence of some wormlike micelles favors local entanglements, and this, in turn, gives rise to the formation of more (Figure 6) and bigger diffusive clusters, which have longer relaxation times (Figure 7). However, as the fast mode does not disappear, spherical or just slightly elongated micelles and wormlike micelles seem to coexist. This result agrees with some TEM pictures in which such coexistence has been found.[48−50]

At $R \approx 0.05$ we observe the appearance of a slow relaxation mode independent of the measurement angle, which indicates that is nondiffusive. This slow mode relaxation time has the same order of magnitude as the one obtained by the viscoelastic measurements, which corresponds to the transient network and could be related, therefore, to scission−reptation Maxwellian relaxation. From these facts, it could be interpreted that the size and concentration of these wormlike micelles is enough to span the whole system and a transient network of wormlike micelles is formed.

When $R \approx 0.1$, the network relaxation time obtained from viscoelastic measurements (τ_M) begins to decrease although G_0, related to the number of entanglements, still increases (see Figure 10). Moreover, the mm still increases too, indicating that the size of the wormlike micelles and diffusive clusters also increases (see mm in Figure 7). The decrease of τ_M tells us that the connecting points of the spanning network formed by the wormlike micelles break apart more and more easily. One possible explanation may be that the amphiphile accumulates preferentially in these connection/branching points inducing a change in curvature. This would create more tension in these regions and would promote a faster disconnection of the network, lowering the network relaxation time, for example, by sliding these connections.

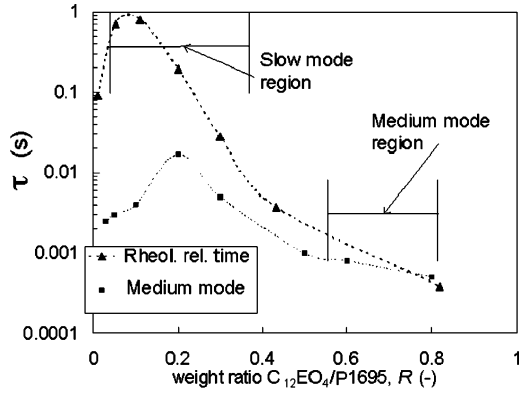

Figure 12. Evolution of rheological relaxation time τ_M and DLS medium mode τ_{mm} with $C_{12}EO_4$/P1695 ratio, *R*.

Above $R \approx 0.2$, although the amount of clusters and wormlike micelles continues to increase (Figure 6) and the number of entanglements begins to reach a plateau (see Figure 10), the incorporation of more amphiphile promotes a decrease in mm relaxation time, indicating a decrease in the size of the wormlike micelles and clusters. This could be due to the fact that when a branching point was almost completely occupied by the surfactant it would prefer to form separated (smaller) disklike micelles or bilayers. A mixture of wormlike micelles that span the network (sm) and wormlike micelles forming local entanglements—diffusive clusters (mm) (with a mixing content of both sucrose surfactant and amphiphile), disklike micelles (with a high content of amphiphilic, mm), and spherical or just slightly elongated micelles (with a high content of sucrose surfactant, fm)—should be present in this region. The dynamic scattering is still dominated by the fast mode at these *R* values (see Figure 6), indicating that the number of monomers/spherical micelles is still very high. Then, one cannot distinguish between the disklike micelles and clusters, both diffusive (only a relatively small and broad medium mode can be observed).

By a further increase of *R*, and the corresponding decrease of wormlike micellar size, a disentanglement of the network is reached that can be observed by the disappearance of the network relaxation slow mode for $R \approx 0.4$. This is somewhat reflected in the viscoelastic measurements because now G' and G'' do not cross each other and only an extrapolation point can be calculated. Then, the scission−reptation relaxation disappears and the system is now dominated again by viscous forces.

In Figure 12 two relaxation times are shown, the relaxation time τ_M, obtained from the Maxwellian fitting of the oscillatory measurements, and the medium mode, τ_{mm}, obtained from DLS. The range in which the slow mode, τ_{sm}, is detected is also indicated. Other authors[51,52] show that the relaxation time of this slow mode, independent of the scattering angle as has been said, is equal to the rheological relaxation time τ_M. Because of the poor time resolution and broad distribution of this slow mode we cannot give an accurate value of the sm relaxation time, but as was stated above, it is of the order of τ_M. In Figure 12 only an estimated range where the sm appears is indicated. It can be seen that the range in which the slow mode is present, that is, when a transient network is formed, is located around the maximum in τ_M.

At high *R* values ($R > 0.5$), when the transient network disappears, the values of τ_M tend to converge with the medium mode, τ_{mm}. It seems, therefore, that the rheology of the system is dominated mainly by the formed spanning network in the region ($0.05 < R < 0.5$), and after that the clusters and disklike micelles responsible for the existence of the medium mode dictate the rheology of the system. Since above $R \approx 0.8$ a lamellar liquid crystal appears, it could be assumed that, at high *R* ratios, most of micelles are disklike or bilayers. The size of these bilayers or "flat aggregates" is ≈40 nm, as can be deduced from the plateau observed from the mm at high *R* values. One can then see the complementarities of both techniques to give an estimation of the structures that could be present in the region of interest around the maximum: the viscoelastic measurements give the relaxation of the network, and the medium mode could give the motion of the clusters and worm or disklike micelles which do not form part of the spanning network. This medium mode relaxation could be considered, also slightly influenced by the fast mode, as the relaxation causing the upturn in G'' at high frequencies (high frequencies from a rheological point of view) when the spanning network is present, and it would be the rheological determinant mode when the network is absent.

5. Conclusions

Sucrose alkanoate surfactants form spherical or slightly elongated micelles in water in the dilute region. The decrease of curvature produced when a short EO-chain polyoxyethylene alkyl ether is added allows the growing of these micelles into wormlike ones, as can be deduced from rheological experiments. When these wormlike micelles are long enough, entanglements between them can take place and a transient network is formed that increases the viscoelasticity of the system. The growing of wormlike micelles is favored when *n* is small. When the amount of C_mEO_n is increased, viscosity and relaxation time also increase, up to a maximum. Further addition of C_mEO_n produces a decrease in them. It is proposed that branching occurs, followed, when more C_mEO_n is added, by the separation of the branching points into disklike micelles or bilayers, precursors of the lamellar liquid crystal phase.

DLS experiments show three relaxation processes: fast-mode, that could be related to the movement of small micelles and surfactant monomers; medium-mode, that we relate to the movement of clusters, wormlike, and/or disklike micelles that are not connected to the network; and a nondiffusive slow-mode, due to the presence of a network produced by entanglements among micelles. The slow mode appears only around the maximum of relaxation time found through rheology, so it is presumably related to this time when a transient network exists. At high *R* values the network disappears, and the rheological relaxation time converges to the medium mode, indicating that rheology is dominated by this mm, probably mostly due to disklike micelles. Further experimentation would, however, be required to prove the proposed mechanism.

We can finally point out that rheology and DLS are useful and complementary techniques for the study of the structure of complex viscoelastic solutions.

References and Notes

(1) Cates, M. E. *J. Phys. Chem.* **1990**, *94*, 371.
(2) Vinson, P. K.; Talmon, Y. *Science* **1990**, *133*, 288.
(3) Edwards, K.; Almgren, N. *J. Colloid Interface Sci.* **1991**, *147*, 1.
(4) Cates, M. E.; Candau, S. J. *J. Phys.: Condens. Matter* **1990**, *2*, 6869.
(5) Rehage, H.; Hoffmann, H. *Mol. Phys.* **1991**, *74*, 933.
(6) Drye, T. J.; Cates, M. E. *J. Chem. Phys.* **1992**, *96*, 1367.
(7) May, S.; Bohbot, Y.; Ben-Shaul, A. *J. Phys. Chem.* **1997**, *101*, 8648.
(8) Candau, S. J.; Hirsch, E.; Zana, R. *J. Colloid Interface Sci.* **1985**, *105*, 521.
(9) Berret, J. F.; Appell, J.; Porte, G. *Langmuir* **1993**, *9*, 2851.
(10) Kern, F.; Lemarechal, P.; Candau, S. J.; Cates, M. E. *Langmuir* **1992**, *8*, 437.

(11) Khatory, A.; Lequeux, F.; Kern, F.; Candau, S. J. *Langmuir* **1993**, *9*, 1456.
(12) Vethamuthu, M. S.; Almgren, M.; Brown, W.; Mukhtar, E. *J. Colloid Interface Sci.* **1995**, *174*, 461.
(13) Kim, W.-J.; Yang, S.-M. *J. Colloid Interface Sci.* **2000**, *232*, 225.
(14) Imai, S.; Shikata, T. *J. Colloid Interface Sci.* **2001**, *244*, 399.
(15) Soltero, J. F. A.; Puig, J. E.; Manero, O. *Langmuir* **1996**, *12*, 2654.
(16) Narayanan, J.; Manohar, C.; Kern, F.; Lequeux, F.; Candau, S. J. *Langmuir* **1997**, *13*, 5235.
(17) Hassan, P. A.; Candau, S. J.; Kern, F.; Manohar, C. *Langmuir* **1998**, *14*, 6025.
(18) Raghavan, S. R.; Kaler, E. W. *Langmuir* **2001**, *17*, 300.
(19) Bandyopadhyay, R.; Sood, A. K. *Langmuir* **2003**, *19*, 3121.
(20) Koehler, R. D.; Raghavan, S. R.; Kaler, E. W. *J. Phys. Chem.* **2000**, *104*, 11035.
(21) Menge, U.; Lang, P.; Findenegg, G. H. *Colloids Surf. A* **2000**, *163*, 81.
(22) Schurtenberger, P.; Mazer, N.; Kanzig, W. *J. Phys. Chem.* **1995**, *99*, 1042.
(23) Hassan, P. A.; Valaulikar, B. S.; Manohar, C.; Kern, F.; Bourdieu, L.; Candau, S. J. *Langmuir* **1996**, *12*, 4350.
(24) Yatcilla, M. T.; Herrington, L.; Brasher, L. L.; Kaler, E. W. *J. Phys. Chem.* **1996**, *100*, 5874.
(25) Raghavan, S. R.; Fritz, G.; Kaler, E. W. *Langmuir* **2002**, *18*, 3797.
(26) Kato, T.; Nozu, D. *J. Mol. Liq.* **2001**, *90*, 167.
(27) Seto, H.; Kato, T.; Monkenbusch, M.; Takeda, T.; Kawabata, Y.; Nagao, M.; Okuhara, D.; Imai, M.; Komura, S. *J. Phys. Chem. Solids* **1999**, *60*, 1371.
(28) Kato, T.; Taguchi, N.; Nozu, D. *Prog. Colloid Polym. Sci.* **1997**, *106*, 557.
(29) Acharya, D. P.; Kunieda, H. *J. Phys. Chem. B* **2003**, *107*, 10168.
(30) Acharya, D. P.; Hossain, Md. K.; Jin-Feng, Sakai, T.; Kunieda, H. *Phys. Chem. Chem. Phys.* **2004**, *6*, 1627.
(31) Gallegos, C.; Muñoz, J.; Guerrero, A.; Berjano, M. *ACS Symp. Ser.* **1994**, *578*, 217.
(32) Rodriguez, C.; Acharya, D. P.; Hinata, S.; Ishitobi, M.; Kunieda, H. *J. Colloid Interface Sci.* **2003**, *262*, 500.
(33) Pes, M. A.; Aramaki, K.; Nakamura, N.; Kunieda, H. *J. Colloid Interface Sci.* **1996**, *159*, 666.
(34) Nakamura, N.; Tagawa, T.; Kihara, K.; Tobita, I.; Kunieda, H. *Langmuir* **1997**, 2001.
(35) Olsson, U.; Shinoda, K.; Lindman, B. *J. Phys. Chem.* **1986**, *90*, 4083.
(36) Furukawa, H.; Horie. K.; Nozaki, R.; Okada, M. *Phys. Rev. E* **2003**, *68*, 031406.
(37) Furukawa, H.; Hirotsu, S. *J. Phys. Soc. Jpn.* **2002**, *71*, 2873.
(38) Blanco, M. C.; Leisner, D.; Vázquez, C.; López-Quintela, M. A. *Langmuir* **2000**, *16*, 8585.
(39) Lequeux, F.; Candau, S. J. *ACS Symp. Ser.* **1994**, *578*, 51.
(40) Manero, O.; Bautista, F.; Soltero, J. F. A.; Puig, J. E. *J. Non-Newtonian Fluid Mech.* **2002**, *106*, 1.
(41) Granek, R.; Cates, M. E. *J. Chem. Phys.* **1992**, *96*, 4758.
(42) Rehage, H.; Hoffmann, H. *J. Phys. Chem.* **1988**, *92*, 4712.
(43) Doi, M.; Edwards, S. F. *The Theory of Polymer Dynamics*; Clarendon: Oxford, UK, 1986.
(44) Oda, R.; Bourdieu, L.; Schmutz, M. *J. Phys. Chem. B* **1997**, *101*, 5913.
(45) Magid, L. H. *J. Phys. Chem. B* **1998**, *102*, 4064.
(46) Rodriguez, C.; Acharya, D. P.; Maestro, A.; Hattori, K.; Aramaki, K.; Kunieda, H. *J. Chem. Eng. Jpn.* **2004**, *37*, 622.
(47) Rouse, P. E. *J. Chem. Phys.* **1953**, *21*, 1272.
(48) Oda, R.; Panizza, P.; Schmutz, M.; Lequeux, F. *Langmuir* **1997**, *13*, 6407.
(49) Lin, Z. *Langmuir* **1996**, *12*, 1729.
(50) Lin, Z.; Cai, J. J.; Scriven, L. E.; Davis, H. T. *J. Phys. Chem. B* **1994**, *98*, 5984.
(51) Nemoto, N.; Kuwahara, M.; Yao, M.-L.; Osaki, K. *Langmuir* **1995**, *11*, 30.
(52) Brown, W.; Johansson, K.; Almgren, M. *J. Phys. Chem.* **1989**, *93*, 5888.